



Yb-doped large mode area fiber for beam quality improvement using local adiabatic tapers with reduced dopant diffusion

YUAN ZHU, MARTIN LEICH*, MARTIN LORENZ, TINA ESCHRICH, CLAUDIA AICHELE, JENS KOBELKE, HARTMUT BARTELT AND MATTHIAS JÄGER

Leibniz Institute of Photonic Technology (IPHT), Albert-Einstein-Str. 9, 07745 Jena, Germany

* martin.leich@leibniz-iph.de

Abstract: A newly designed all-solid step-index Yb-doped aluminosilicate large mode area fiber for achieving high peak power at near diffraction limited beam quality with local adiabatic tapering is presented. The 45 μ m diameter fiber core and pump cladding consist of active/passively doped aluminosilicate glass produced by powder sinter technology (REPUSIL). A deliberate combination of innovative cladding and core materials was aspired to achieve low processing temperature reducing dopant diffusion during fiber fabrication, tapering and splicing. By developing a short adiabatic taper, robust seed coupling is achieved by using this Yb-doped LMA fiber as final stage of a nanosecond fiber Master Oscillator Power Amplifier (MOPA) system while maintaining near diffraction limited beam quality by preferential excitation of the fundamental mode. After application of a fiber-based endcap, the peak power could be scaled up to 375 kW with high beam quality and a measured M^2 value of 1.3~1.7.

© 2018 Optical Society of America under the terms of the [OSA Open Access Publishing Agreement](#)

OCIS codes: (060.2280) Fiber design and fabrication; (060.2290) Fiber materials; (060.2320) Fiber optics amplifiers and oscillators; (140.3280) Laser amplifiers.

References and links

1. D. J. Richardson, J. Nilsson, and W. A. Clarkson, "High power fiber lasers: current status and future perspectives [Invited]," *J. Opt. Soc. Am. B* **27**(11), B63–B92 (2010).
2. F. J. Duarte, *Tunable Laser Applications* (CRC, 2008).
3. G. P. Agrawal, *Nonlinear Fiber Optics* (Elsevier, 2013).
4. C. Jauregui, J. Limpert, and A. Tünnermann, "High-power fibre lasers," *Nat. Photonics* **7**(11), 861–867 (2013).
5. R. M. Wood, *Laser-Induced Damage of Optical Materials* (Institute of Physics Publishing, 2003).
6. D. Jain, Y. Jung, J. Kim, and J. K. Sahu, "Robust single-mode all-solid multi-trench fiber with large effective mode area," *Opt. Lett.* **39**(17), 5200–5203 (2014).
7. P. Wang, L. J. Cooper, J. K. Sahu, and W. A. Clarkson, "Efficient single-mode operation of a cladding-pumped ytterbium-doped helical-core fiber laser," *Opt. Lett.* **31**(2), 226–228 (2006).
8. C. Liu, G. Chang, N. Litchinitser, A. Galvanauskas, D. Guertin, N. Jabobson, and K. Tankala, "Effectively Single-Mode Chirally-Coupled Core Fiber," in *Advanced Solid-State Photonics*, OSA Technical Digest Series (CD) (Optical Society of America, 2007), paper ME2.
9. T. A. Birks, J. C. Knight, and P. St. J. Russell, "Endlessly single-mode photonic crystal fiber," *Opt. Lett.* **22**(13), 961–963 (1997).
10. L. Dong, X. Peng, and J. Li, "Leakage channel optical fibers with large effective area," *J. Opt. Soc. Am. B* **24**(8), 1689–1697 (2007).
11. J. Limpert, F. Stutzki, F. Jansen, H. J. Otto, T. Eidam, C. Jauregui, and A. Tünnermann, "Yb-doped large-pitch fibres: effective single-mode operation based on higher-order mode delocalization," *Light Sci. Appl.* **1**(4), e8 (2012).
12. R. Dauliat, A. Benoît, D. Darwich, R. Jamier, J. Kobelke, S. Grimm, K. Schuster, and P. Roy, "Demonstration of a homogeneous Yb-doped core fully aperiodic large-pitch fiber laser," *Appl. Opt.* **55**(23), 6229–6235 (2016).
13. C. D. Brooks and F. Di Teodoro, "Multimegawatt peak-power, single-transverse-mode operation of a 100 μ m core diameter, Yb-doped rodlike photonic crystal fiber amplifier," *Appl. Phys. Lett.* **89**(11), 111119 (2006).
14. C. Gaida, F. Stutzki, F. Jansen, H.-J. Otto, T. Eidam, C. Jauregui, O. de Vries, J. Limpert, and A. Tünnermann, "Triple-clad large-pitch fibers for compact high-power pulsed fiber laser systems," *Opt. Lett.* **39**(2), 209–211 (2014).

15. M. Y. Cheng, Y. C. Chang, A. Galvanauskas, P. Mamidipudi, R. Changkakoti, and P. Gatchell, "High-energy and high-peak-power nanosecond pulse generation with beam quality control in 200-microm core highly multimode Yb-doped fiber amplifiers," *Opt. Lett.* **30**(4), 358–360 (2005).
16. C. Ye, S. Honkanen, J. Montiel i Ponsoda, A. Tervonen, T. Kokki, and J. Koponen, "Near-diffraction-limited output from confined-doped ytterbium fibre with 41 μm core diameter," *Electron. Lett.* **47**(14), 819–821 (2011).
17. V. Filippov, Y. Chamorovskii, J. Kerttula, K. Golant, M. Pessa, and O. G. Okhotnikov, "Double clad tapered fiber for high power applications," *Opt. Express* **16**(3), 1929–1944 (2008).
18. K. Bobkov, A. Andrianov, M. Koptev, S. Muravyev, A. Levchenko, V. Velmiskin, S. Aleshkina, S. Semjonov, D. Lipatov, A. Guryanov, A. Kim, and M. Likhachev, "Sub-MW peak power diffraction-limited chirped-pulse monolithic Yb-doped tapered fiber amplifier," *Opt. Express* **25**(22), 26958–26972 (2017).
19. V. Filippov, A. Vorotyanski, T. Noronen, R. Gumenyuk, Y. Chamorovskii, and K. Golant, "Picosecond MOPA with ytterbium doped tapered double clad fiber," *Proc. SPIE* **10083**, 100831H (2017).
20. A. Fedotov, T. Noronen, R. Gumenyuk, V. Ustimchik, Y. Chamorovskii, K. Golant, M. Odnoblyudov, J. Rissanen, T. Niemi, and V. Filippov, "Ultra-large core birefringent Yb-doped tapered double clad fiber for high power amplifiers," *Opt. Express* **26**(6), 6581–6592 (2018).
21. Y. Zhu, T. Eschrich, M. Leich, S. Grimm, J. Kobelke, M. Lorenz, H. Bartelt, and M. Jäger, "Yb³⁺-doped rod-type amplifiers with local adiabatic tapers for peak power scaling and beam quality improvement," *Laser Phys.* **27**(10), 105103 (2017).
22. D. Marcuse, "Loss analysis of single-mode fiber splices," *Bell Syst. Tech. J.* **56**(5), 703–718 (1977).
23. R. P. Photonics Encyclopedia, "V Number", https://www.rp-photonics.com/v_number.html.
24. J. Kirchhof, S. Unger, and J. Dellith are preparing a manuscript to be called "The viscosity of fluorine-doped silica glasses."
25. S. Jetschke, S. Unger, M. Leich, and J. Kirchhof, "Photodarkening kinetics as a function of Yb concentration and the role of Al codoping," *Appl. Opt.* **51**(32), 7758–7764 (2012).
26. S. Jetschke, S. Unger, A. Schwuchow, M. Leich, and M. Jäger, "Role of Ce in Yb/Al laser fibers: prevention of photodarkening and thermal effects," *Opt. Express* **24**(12), 13009–13022 (2016).
27. K. Schuster, S. Unger, C. Aichele, F. Lindner, S. Grimm, D. Litzkendorf, J. Kobelke, J. Bierlich, K. Wondraczek, and H. Bartelt, "Material and technology trends in fiber optics," *Adv. Opt. Technol.* **3**(4), 447–468 (2014).
28. M. Leich, F. Just, A. Langner, M. Such, G. Schötz, T. Eschrich, and S. Grimm, "Highly efficient Yb-doped silica fibers prepared by powder sinter technology," *Opt. Lett.* **36**(9), 1557–1559 (2011).
29. M. Leich, U. Röpke, S. Jetschke, S. Unger, V. Reichel, and J. Kirchhof, "Non-isothermal bleaching of photodarkened Yb-doped fibers," *Opt. Express* **17**(15), 12588–12593 (2009).
30. J. D. Love, W. M. Henry, W. J. Stewart, R. J. Black, S. Lacroix, and F. Gonthier, "Tapered single-mode fibres and devices," in *Proceedings of IEEE J* **138**, 343–354 (1991).
31. A. Wetter, M. Faucher, B. Sévigny, and N. Vachon, "High core and cladding isolation termination for high-power lasers and amplifiers," *Proc. SPIE* **7195**, 719521 (2009).
32. J. Limpert, S. Höfer, A. Liem, H. Zellmer, A. Tünnermann, S. Knoke, and H. Voelckel, "100-W average-power, high-energy nanosecond fiber amplifier," *Appl. Phys. B* **75**(4-5), 477–479 (2002).

1. Introduction

Many industrial applications in laser materials processing require mechanically robust laser systems with high beam quality (close to diffraction limited) and high peak power (~1MW) [1,2]. In comparison with other types of high power solid-state lasers, fiber lasers have attracted a lot of attention and experienced rapid development in the last 20 years due to their numerous advantages such as alignment-free operation, robustness, high efficiency, excellent thermal management and superior beam quality at high power. But peak power scaling for standard fiber amplifier is still limited because of parasitic nonlinear effects due to small mode field diameters and long effective interaction lengths [3,4], and low facet damage threshold due to high intensity [5].

An efficient solution to solve this problem is scaling up the mode field diameter (MFD) of the active fiber to suppress nonlinear effects and increase facet damage threshold due to the reduction of the local power intensity. In order to maintain single-mode operation in large mode area (LMA) fibers, several special techniques have been proposed such as multi-trench fiber [6], helical core fiber [7], chirally coupled core fiber [8], photonic crystal fiber (PCF) [9], leakage channel fiber [10] and large pitch fiber (LPF) [11,12]. Among all these proposals, the concepts of active PCF and LPF have been successful in scaling up the peak power to the megawatt (MW) level and even to the self-focusing limit (4MW) [13]. But due to their air hole structure and complexity of refractive index matching of the active core to the cladding,

especially for high Yb concentrations [14], these special fiber types are quite expensive, challenging in processing and in achieving robustness with respect to the seed coupling.

Consequently, all-solid step-index LMA fibers become an economical and practical option to adopt. Several methods have been proposed to maintain good beam quality with all-solid LMA fibers such as coiled fiber [15], confined doped fiber [16] and the adiabatic tapering for modal control [17–21]. Bobkov et al. [18] have investigated long tapered fiber amplifiers in parallel with our research work at recent years. Up to now, they achieved over 0.76MW peak power directly from a 2m long tapered fiber amplifier. Filippov et al. have done a series of research work with several meters long tapered fiber in recent years [17,19,20]. They have achieved 5MW peak power and perfect beam quality with the use of a picosecond MOPA with double clad ytterbium doped tapered fiber (4m length) in 2017 [19]. But the authors had to face two serious problems: significant ASE and Raman emission. The latest publication of this group in 2018 [20] shows a 3.6m long Yb-doped tapered double clad fiber, which provides an amplification up to 28W with 292kW peak power and a spectrum free of Raman components in the case of 90ps at 1MHz repetition rate.

Almost all these published research works with tapered fiber use several meters long tapers. This kind of long taper is produced during the fiber drawing process by quickly varying the fiber drawing parameters. However, it is difficult to precisely control the taper drawing condition and tapering ratio is limited. In addition, long active fiber length (including taper and fiber) can decrease optical power limits of several unwanted parasitic non-linear effects such as Stimulated Raman Scattering (SRS) or Stimulated Brillouin Scattering (SBS). Therefore, short local adiabatic taper is an urgent need to suppress unwanted non-linear effects for extremely high peak power. In our previous work, we have introduced the application of short local adiabatic tapers (5cm taper length) with LMA fibers (46cm rod fiber length) for peak power scaling while maintaining good beam quality. For this purpose, a large-core step-index fiber with very high Yb (0.6mol% Yb_2O_3) and Al doping (9mol% Al_2O_3) was investigated to achieve high pump absorption and NA with respect to a pure silica cladding [21]. Diffusion during tapering and splicing is observed, which limits the achievable beam quality to M^2 values near 3.5.

In this research work, we present our local short taper approach with a newly designed Yb-doped aluminosilicate fiber with 72cm fiber length including a 5cm taper), which has been optimized in terms of reducing diffusion during tapering and splicing. This is achieved by reducing the Al^{3+} concentration in the fiber core and pump cladding and the additional application of a highly fluorinated (F)-doped cladding tube lowering the viscosity and therefore the processing temperature and diffusion in the fiber. The fiber design has also to be adapted to the requirements for adiabatic tapering and splicing to the MOPA system. In this context, the influence of the fiber NA is discussed. Using the local adiabatic taper approach, fiber drawing and tapering process are decoupled, providing more flexibility on the taper design and keeping the drawing process simple. To achieve high peak power, we apply an endcap at the fiber consisting of a short silica fiber piece.

2. Tapered LMA fiber design

Figure 1 is showing the main features of a tapered LMA fiber amplifier with double clad structure: (1) The splice between seed delivery fiber and taper waist is very important and determines the power coupling efficiency. The waist of the tapered active fiber needs to be single-mode at the splice to avoid higher order modes (HOMs) excitation. (2) The adiabatic taper is the key component to maintain single mode operation in LMA fiber. An adiabatic taper means that the taper geometry varies smoothly enough that no power is coupled between the fundamental mode (FM) and the HOMs. The essence of this approach is utilizing the local adiabatic taper to provide a monolithic signal path and selectively excite the FM of a highly multimode fiber. (3) A homogeneous refractive index profile of the LMA fiber core is

also very important to achieve a near Gaussian mode field distribution, because any variation can influence the beam quality due to mode distortion in LMA fibers.

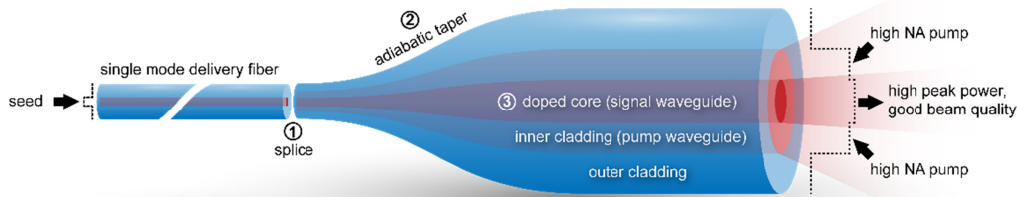


Fig. 1. Tapered fiber amplifier setup with double clad fibers structure.

In order to estimate the required mode field diameter (MFD) of the LMA fiber, the typical optical limits (Self focusing, Stimulated Raman Scattering (SRS) and Facet damage threshold) [3,5] are plotted in Fig. 2 where it is assumed that the effective fiber length corresponds to 0.2m of the real active fiber length [3]. The MFD of the rod-type fiber used in this research work is $31\mu\text{m}$, which allows scaling up the peak power to the surface damage threshold of 380kW and up to the SRS limit of 660kW, if an endcap is adopted to enhance the surface damage threshold.

2.1 Design aspects of LMA fiber amplifier: seed splice

Our approach is to apply a local short adiabatic taper to an LMA fiber, which is directly spliced to the seed delivery fiber of a Master Oscillator Power Amplifier (MOPA) system. In order to achieve the maximum signal power coupling without HOMs excitation, two criteria should be met: (1) mode matching at the splice between seed delivery fiber and taper waist should be satisfied, and (2) the taper waist should be single mode to avoid HOMs excitation.

In Fig. 3 the MFD is plotted as a function of the fiber core diameter for different values of the numerical aperture (NA). The MFD was estimated with Marcuse's equation [22] assuming that mainly the single-mode region with V-parameter ≤ 2.405 is subject of the following discussion: The seed delivery fiber has a core diameter of $10\mu\text{m}$, MFD of $11\mu\text{m}$ and a core NA of 0.08. If the core NA of the rod type fiber is too small e.g. NA = 0.04, the MFD of the taper waist will be quite large (larger than $21\mu\text{m}$), compared with the seed delivery fiber. In this case, the MFD of taper waist and the seed delivery fiber cannot match well and the power coupling loss will be high. If the core NA of the rod type fiber is too large e.g. NA = 0.12, the calculated curve in Fig. 3 has two crossing points where the MFD is $11\mu\text{m}$: The first one for (small core diameter) is in a critical region where the MFD varies significantly with core diameter. The second one is in the region where the V number of taper waist, which is a normalized frequency parameter, determining the number of modes of a step-index fiber [23] is larger than 2.405 (single mode criterion). This could result in an excitation of HOMs at the splice. Therefore, the core NA of the active fiber should be around 0.08 to achieve the best mode matching between seed delivery fiber and taper waist. The V number of the taper waist should be below 2.405 to avoid the HOMs excitation.

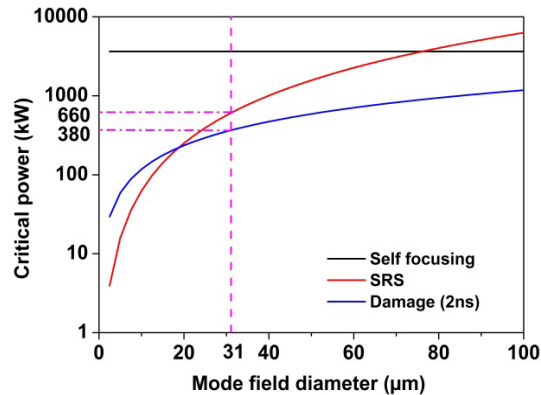


Fig. 2. Critical power limits as a function of MFD.

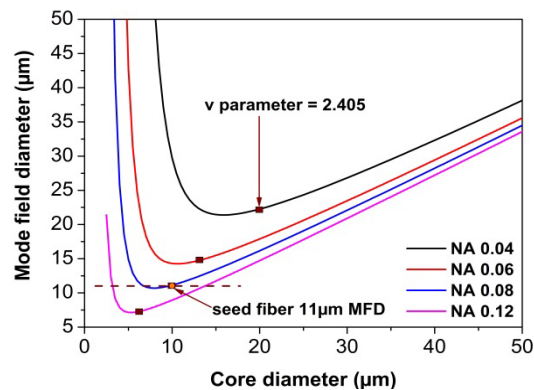


Fig. 3. Mode field diameter for different core diameters and core NA.

2.2 Optimized fiber design to suppress the dopant diffusion

The inner cladding of the active fiber (pump cladding) is co-doped with Al_2O_3 on the one hand to adjust the core NA of the fiber to 0.08 and on the other hand to increase the pump NA with respect to the outer F-doped silica cladding. In our previous work [21], it was found that dopants diffusion between fiber core and inner cladding, which have been heavily co-doped with Al_2O_3 happens during the high temperature tapering and splicing process. This can remarkably change the properties of the fiber and limit the achievable beam quality.

In order to mitigate the influence of diffusion, several improvements were introduced with this newly designed rod-type fiber including (1) the reduction of Al^{3+} -content in the fiber core and the inner cladding to 2.5 and 3mol%, respectively and (2) the reduction of the glass transition temperature of the outer cladding to reduce the process temperature during tapering. The latter can be achieved by using a highly F-doped cladding tube (Heraeus F520-42, corresponding to 1.2mol% SiF_4). According to [24], the glass viscosity and therefore the fiber drawing and tapering temperature are remarkably decreased for higher Fluorine dopant concentrations. A typical value for kinematic similar fiber drawing conditions is a temperature reduction of about 60 K – 80 K for F520 preforms in comparison with pure silica preforms.

To achieve high pump absorption that is necessary to minimize the active fiber length and therefore limit nonlinear effects, a high Yb_2O_3 content (0.25mol%) and large core-to-clad diameter ratio (CCDR) is necessary. For efficient photodarkening mitigation sufficient Al_2O_3 and Ce_2O_3 co-doping is required [25,26]. Another important aspect is the homogeneity of the

REPUSIL core glass. Small inhomogeneities or index fluctuations that scatter signal light can disturb the fundamental mode and have to be avoided to achieve a small M^2 value.

3. Experiment results

3.1 Preform and fiber fabrication

For preparation of the preform, an active and passive REPUSIL glass was prepared by powder-sinter technology [27,28] and drawn into rods of 1 mm outer diameter. This technology allows providing large actively and passively doped glass rods with very uniformly distributed dopants resulting in high index homogeneity [28]. The active core glass contains 0.25mol% Yb_2O_3 , 0.2mol% Ce_2O_3 and 2.5mol% Al_2O_3 and the passive inner cladding contains 3mol% Al_2O_3 . The fiber preform was prepared by hexagonal stacking of a central Yb-doped rod with 2 rings of Al-doped passive rods and overcladding them twice with a highly F-doped outer cladding tube F520-42 (Heraeus Quarzglas GmbH). Finally, a rod-type double-clad fiber with 45 μm core diameter, a 200 μm inner cladding, and a 785 μm outer diameter [Fig. 4(a)] was drawn. Dimensions were measured by software analysis of a camera picture from a Zeiss microscope (Zeiss, AXIO Imager.M1m). An additional test fiber with 150 μm outer diameter was drawn for fundamental characterization and photodarkening measurement.

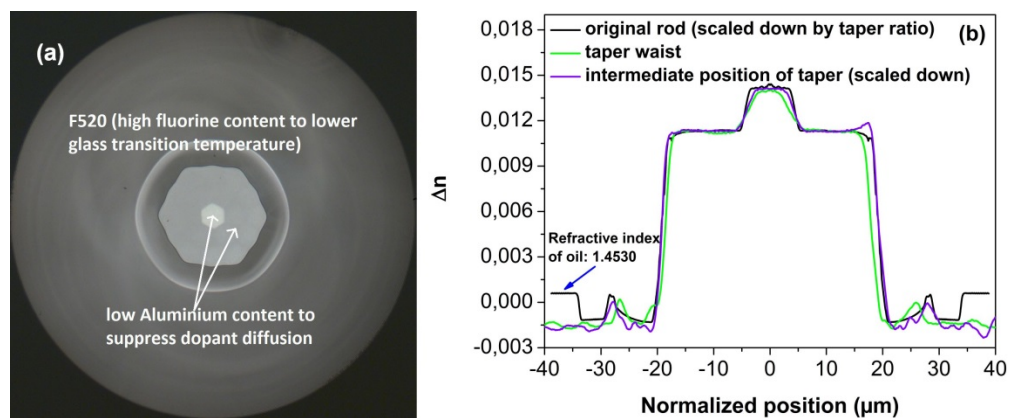


Fig. 4. (a) Cross-section of LMA fiber (Yb/Al/Ce-doped core, Al-doped inner cladding and outer cladding with highly fluorine doped silica tube to lower glass transition temperature). (b) Refractive index profile of rod-type fiber and its down-taper with reduced diffusion.

In order to measure the refractive index (RI) profile using an Interfiber Analysis IFA-100 index profilometer, the rod-type fiber is etched to 400 μm outer diameter. The result shows that the fiber made by REPUSIL achieved a very homogenous step index profile with a core NA of 0.09 and a pump NA of 0.19. The latter is remarkable, because the relatively high pump NA was achieved without plasma outside deposition (POD) due to the up-doping of the inner cladding with Al_2O_3 . In order to check if this fiber exhibits significant diffusion, the refractive index of the down taper is measured at two positions [Fig. 4(b)]. When comparing these down taper RI profiles with the RI profile of the rod fiber (all scaled down to the same core diameter), there is only little difference between them, which means that the diffusion phenomenon even during tapering is successfully mitigated.

To ensure that our developed core material has low photodarkening (PD), we have measured the temporal PD loss with a standard technique [29] with 200mW core-pumping at 976nm at a 2cm short fiber sample. The resulting loss curve is shown in Fig. 5. The measured loss value of 11dB/m and the fitted equilibrium value of 25.4dB/m are very low compared to fibers with similar ytterbium/aluminum content and without cerium [25].

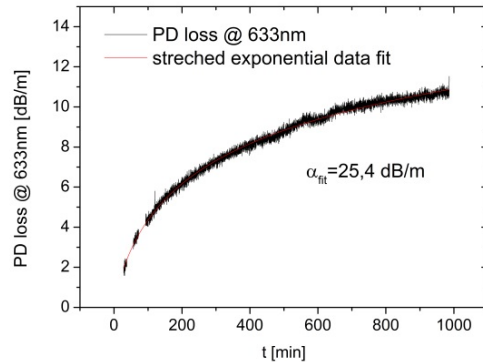


Fig. 5. Temporal photodarkening measurement at test fiber showing low photodarkening loss.

3.2 Preparation of local adiabatic short tapers

The taper was fabricated with the help of a single direction taper process of the Vytran GPX3200. The heat source of the device is a resistance heater in shape of an inverse Omega consisting of a graphite filament with 3 mm in width. The taper made for the amplifier has the following typical dimensions: the downtaper including a part of the waist is about 50mm long.

The fabricated tapers were scanned by a 3SAE LDS 2, which has a tool to measure the outer diameter of a taper in two orthogonal projections. If it can be assumed that there is negligible diffusion during tapering the core diameter can be determined via ratio equation of outer and core diameter of the fiber. After tapering the waist was cleaved and spliced to the seed fiber in order to couple the seed signal into the amplifier rod. Some effort was put into the alignment of the two fibers to avoid any unwanted coupling into higher order modes (HOM) already at the splice position“.

Figure 6(a) shows the measured outer taper diameter versus the taper length. Figure 6(b) shows the theoretical calculation of local taper angle of the core, black line as derived from the real taper shape [Fig. 6(a)], assuming the core diameter changes proportionally to the outer diameter. The other colored curves show the adiabatic limit for coupling of the fundamental mode to the next three higher order modes according to the adiabatic taper length criterion [30]. The experimentally realized taper angle is always smaller than the adiabatic threshold which means the taper shape should be smooth enough that the FM profile can smoothly evolve inside the taper core, theoretically without power coupling between the FM and the HOMs.

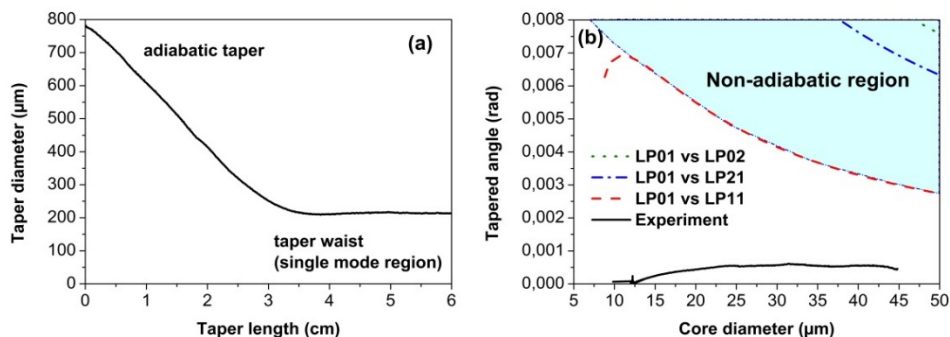


Fig. 6. (a) Scanned taper length and outer diameter (b) Comparison of angular profiles between the experimentally realized fiber taper and the adiabatic thresholds.

3.3 Tapered LMA amplifier results and discussion

A three-stage fiber-based MOPA system with flexible pulse parameters was adopted, choosing a 2ns pulse width and 20kHz repetition rate for the amplifier characterization [21]. The two pre-amplifier stages provide 138mW of average power and 3kW of peak power as seed for the third amplifier stage. The third stage of MOPA system is the main stage to test the designed LMA fibers, which are counter-pumped at a wavelength of 976nm. We have used a high brightness wavelength stabilized multimode pump diode with NA = 0.15 and 105 μ m core output fiber. Free space seed coupling is used for a non-tapered reference fiber, while the tapered fiber is directly spliced to the MOPA system for monolithic seed coupling.

Two fiber samples are characterized including the non-tapered reference fiber (62cm) and the tapered fiber with 72cm length including a 5cm taper [Fig. 6(a)]. The measured slope efficiency of 72% for both cases is achieved with respect to the absorbed pump power (Fig. 7). Here, the launched pump power is estimated based on 90% pump coupling efficiency, the residual pump power for the tapered fiber amplifier is estimated according to a constant absorption coefficient along the fiber, which is obtained from the non-tapered fiber amplifier. The highest extracted output power is 13.8W with 210kW peak power for the non-tapered reference fiber, while the highest output power is 8.4W with 140kW peak power for tapered fiber. Both of them are limited by the facet damage.

In order to enhance the damage threshold and scale up the peak power of the tapered fiber amplifier, an endcap is adopted to protect the fiber facet from facet damage [31,32]. For endcap material we employ an F300 silica rod with 1mm outer diameter. The silica rod was spliced to the tapered fiber amplifier and angle-cleaved with 5.8 degrees at a length of only 2mm to avoid back-reflections into the MOPA system and to ensure efficient pump coupling at the same time (Fig. 8). To adopt this endcap, several trials of splicing and cleaving were necessary and resulted in an amplifier length of 50cm (45cm rod and 5cm taper) for further investigations on the same tapered rod fiber.

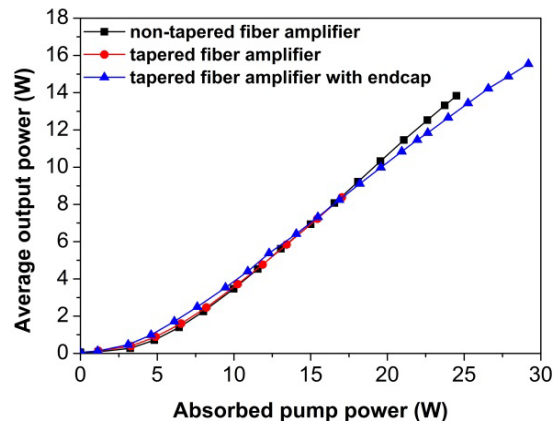


Fig. 7. Average output power versus the absorbed pump power.

The slope efficiency of this 50cm length tapered amplifier displays a value of 62% vs. the absorbed pump power (Fig. 7). The highest output power reached 15.5W under 39.5W of incident pump power, corresponding to a peak power of 375kW and pulse energy of 0.78mJ. The main reason for the slightly reduced efficiency compared to the previous samples is the shorter active fiber length (reduced by 22cm), because taper and seed coupling have not changed.

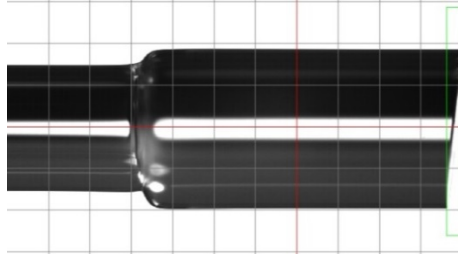


Fig. 8. Endcap of the tapered fiber amplifier: the left side is the fiber amplifier and the right side is the endcap material (F300 with 1mm outer diameter and 5.8 degrees cleave angle).

The spectrum of the amplified signal with 375kW peak power is shown in Fig. 9 and is compared to the spectrum of the seed source. The seed spectrum already contains a significant first Stokes peak at 1080nm due to SRS. This SRS peak is efficiently suppressed in the tapered rod amplifier up to 375kW of peak power, which indicates that the Raman gain is still very small while the laser gain strongly favors the 1030nm emission. The spectrum around 1030nm becomes broader than the seed spectrum which is due to the nonlinear broadening effect.

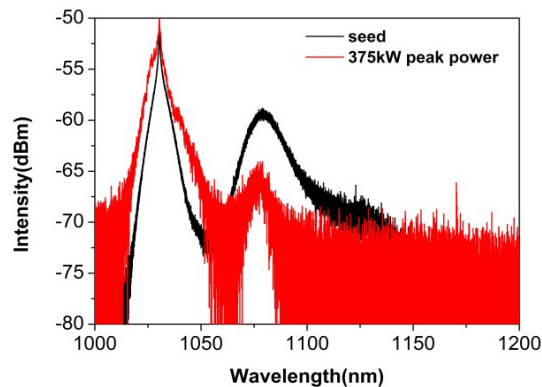


Fig. 9. Normalized optical spectrum of seed and amplified light of the end-capped amplifier, indicating that the amplifier is running still far away from the SRS limit.

The beam quality was measured using a Spiricon M2-200s. The measured values are plotted versus the average output power in Fig. 10. The non-tapered rod amplifier and the tapered fiber amplifier without endcap serve as a reference. For this tapered fiber amplifier with endcap, the measured M^2 values are ranging from 1.3 to 1.7 in the nearly diffraction limited, which is very similar to the tapered fiber amplifier without endcap. For highest average output power of about 14W, the beam quality is improved from values near 3.5 with non-tapered fiber to 1.5 with tapered fiber showing a significant improvement. For the tapered fiber an example for the intensity distribution in the far field is plotted in the inset of Fig. 10. The profile is showing a nearly Gaussian distribution.

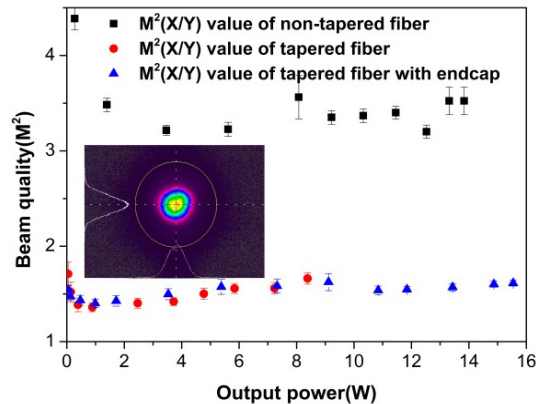


Fig. 10. Measured beam quality for the non-tapered reference fiber amplifier, the tapered fiber amplifier and the tapered fiber amplifier with endcap; inset: far field intensity distribution of output beam for the tapered fiber.

4. Conclusion

In summary, we have demonstrated a new design of a 45 μm core diameter LMA Yb-doped step-index fiber that is well suited for local adiabatic tapering with reduced diffusion effects. Our tapered REPUSIL-based rod-type amplifier allows efficient high peak power amplification of ns pulses in combination with near diffraction limited beam quality in a robust monolithic seed coupling setup.

A moderate Al^{3+} -content for core and inner cladding helps to mitigate diffusion during tapering. In addition, by applying a highly F-doped silica tube for the outer cladding the glass viscosity of the fiber is decreased resulting in lower fiber drawing and tapering process temperatures. While a non-tapered fiber amplifier was operated up to a peak power of 210kW, the tapered amplifier reached 140kW with an efficiency of 72%. In both cases peak power was limited by damage of the end-facet. For the tapered fiber the threshold was lowered due to the better M^2 value resulting in a smaller effective MFD and therefore a higher pulse energy density at the end facet. Both fiber amplifiers show relatively low SRS levels and no remarkable photodarkening. The measured M^2 values for the tapered rod are between 1.3 and 1.7 with much higher stability compared to the free space coupling of the non-tapered fiber. Owing to the application of a fiber-based endcap, the peak power of the tapered fiber amplifier could be significantly scaled up to 375kW, which is 2.7 times higher than for the tapered fiber without endcap.

We expect further improvements with respect to higher beam quality resulting from future developments of improved index matching and homogenization of the REPUSIL glass. For higher peak power scaling picosecond pulses are a promising concept, especially because of their lower surface damage threshold.

Funding

M-Eranet project Surlas from the German Federal Ministry of Education and Research (BMBF, FKZ 13N13683); China Scholarship Council (201206380069).

Acknowledgments

The IFA-100 as a basic tool for this research work was funded by the Free State of Thuringia under the project number 2015-0021. We also thank Ron Fatobene for helping with the creation of the graphics.